Discrimination of cloud and aerosol in the Stratospheric Aerosol and Gas Experiment III occultation data

Geoffrey S. Kent, Pi-Huan Wang, and Kristi M. Skeens

The Stratospheric Aerosol and Gas Experiment (SAGE) III, scheduled for a first launch in mid-1998, will be making measurements of the extinction that is due to aerosols and gases at many wavelengths between 385 and 1550 nm. In the troposphere and wintertime polar stratosphere, extinction will also occur because of the presence of cloud along the optical path from the Sun to the satellite instrument. We describe a method for separating the effects of aerosol and cloud using the extinction at 525, 1020, and 1550 nm and present the results of simulation studies. These studies show that the new method will work well under background nonvolcanic aerosol conditions in the upper troposphere and lower stratosphere. Under conditions of severe volcanic contamination, the error rate for the separation of aerosol and cloud may rise as high as 30%.

Key words: Satellite occultation measurements, Stratospheric Aerosol and Gas Experiment (SAGE) III, upper-tropospheric cloud, cloud discrimination.

1. Introduction

The Stratospheric Aerosol and Gas Experiment (SAGE) III will be the latest in the series of solar occultation satellites designed to measure stratospheric and upper-tropospheric aerosols and trace gases.[1,2] The instrument is currently manifested onboard a polar-orbiting Meteor-3M satellite and the International Space Station, with the first flight scheduled for 1998. Although not specifically designed for the study of cloud, the SAGE III predecessors have shown themselves to be extremely valuable in the study of the climatology of high cloud, particularly the thinner subvisual component. These studies have led to the archival of maps of the global high-cloud distribution for various altitudes and times at the Langley Distributed Active Archive Center.

SAGE II, currently operating, and the immediate predecessor of SAGE III, measures aerosol extinction along a horizontal path through the atmosphere at four wavelengths (385, 435, 525, and 1020 nm). Of these, only the two longest wavelengths have an appreciable penetration into the troposphere, and data at these wavelengths have been used to determine the frequency of cloud occurrence. The distinction of the attenuation that is due to cloud from that due to aerosols has been based on the differential variation of extinction with wavelength by use of the values of the extinction obtained at wavelengths 525 and 1020 nm. This method relies on the fact that aerosols are generally small in size compared with the wavelengths, producing a significant variation of extinction with wavelength (the extinction at 525 nm is typically a factor of 2–5 greater than that at 1020 nm). In contrast, cloud particles are much larger, producing little or no wavelength variation of extinction. The method is found to work well in the upper troposphere, except that after the injection of material from volcanic eruptions, particles form that are large compared with those associated with the background aerosol.[3]

SAGE III will extend the capabilities of the earlier instruments. It is currently designed to make aerosol measurements at wavelengths of 385, 450, 525, 670, 757, 872, 1020, and 1550 nm. The new longer wavelengths will provide additional data in the troposphere, and, in the absence of cloud, data will be obtained at the two longest wavelengths down to the surface of the Earth. Furthermore, data obtained at the 1550-nm wavelength will provide increased discrimination for cloud against the larger aerosols. In contrast to the current situation with SAGE II, cloud presence will become a primary data product of SAGE III. In this paper we describe how data at the

The authors are with the Science and Technology Corporation, 101 Research Drive, Hampton, Virginia 23666-1340.

Received 6 February 1997; revised manuscript received 4 August 1997.

0003-6935/97/338639-11$10.00/0

1550-nm wavelength can be used to assist in the separation of the signature of cloud from that of aerosol, particularly when volcanic aerosols are present. The results of simulation studies carried out with the results of *in situ* measurements of aerosol concentrations and sizes are presented. An intercomparison is also made between the relative performance of the older discrimination methods used with SAGE II data and those proposed for use with SAGE III data.

SAGE II makes measurements at more than one wavelength for altitudes of 6 km or greater. SAGE III will make two wavelength (1020-nm and 1550-nm) measurements down to the surface of the Earth, offering the possibility of using these two wavelengths to discriminate aerosol from cloud at all altitudes. At lower altitudes large aerosols similar in size to those of recent volcanic origin will be present; these aerosols will be of more complex composition than those of volcanic origin and may also be nonspherical. These characteristics may make uncertain any aerosol–cloud separation method that is based on the variation of extinction with wavelength. We do not discuss this problem in this paper. Rather, we use data from three wavelengths (525, 1020, and 1550 nm), the shortest of which provides data at altitudes above 6 km only. We are thus concerned with the use of the additional wavelength information (as compared with SAGE II) to provide improved discrimination between aerosols and cloud for altitudes above 6 km.

The aerosol–cloud separation methods discussed below are simplistic. They ignore effects that are due to cloud geometry and the curvature of the Earth, and they accept the assumption of horizontal homogeneity that is built into the SAGE II cloud inversion scheme. These simplifications may cause errors to arise in the determination of cloud altitude and extinction but do not affect the determination of whether cloud is present along the optical path from the Sun to the satellite instrument. Some of the consequences of our making these assumptions are discussed in more detail in Section 7, where the main effects resulting from the inhomogeneous nature of cloud are described.

2. Cloud and Aerosol Separation in SAGE II Data

A. Opaque Cloud

The aerosol–cloud separation methods described in the following sections assume that radiation is received at the satellite from the Sun at all three wavelengths used (525, 1020, and 1550 nm). This is not always the case. Inversion of extinction data at 525 nm is stopped at a tangent altitude of 6.5 km because of the low signal levels below that altitude. Most extinction profiles at 1020 nm do not reach to the Earth's surface because of excessive attenuation of the signal, and similar behavior is to be expected for the 1550-nm channel on SAGE III. Such termination occurring in the upper troposphere or in the polar stratosphere is thought to be due to the presence of opaque cloud along the optical path from the Sun to the satellite instrument. The equivalent vertical optical depth of the cloud for which termination just occurs depends on the cloud geometry but is of the order of 0.05 (i.e., the cloud is thin but not subvisual). At times of high-volcanic aerosol content, such as that following the Mount Pinatubo volcanic eruption, the extinction produced by the volcanic aerosol may also be large enough to cause profile termination,[4] sometimes at considerable altitudes. At nonvolcanic times these occurrences are thought to be due only to cloud, the altitude assigned to the cloud being 1.0 km (0.5 km for SAGE III) below that of the last data point on the profile. For tangent altitudes occurring below and within a few kilometers of the tropopause, the number of terminating profiles is found to be considerably fewer than the number of profiles showing nonopaque cloud. As we proceed to lower altitudes, the number of terminating profiles increases markedly. Occasionally a profile may terminate at one or two wavelengths only, even for altitudes above 6 km. In such cases cloud presence is not possible to determine.

B. Nonopaque Cloud

Earlier analyses of SAGE II cloud data[5–7] relied on the fact that the extinction that was due to cloud occurring along the optical path from the Sun to the satellite instrument was likely to be much greater than that due to aerosol. An arbitrary extinction level was set, and all extinction values greater than this level were attributed to the presence of cloud. Although useful information was obtained about the global distribution of thin high cloud by these methods, problems were encountered at certain latitudes and times because of the variable nature of the aerosol extinction, which could on occasion rise above the discrimination level. Comparison of the cloud distributions obtained from these analyses with those obtained by other researchers using different instruments showed good agreement with respect to the regions of maximum cloud and seasonal variations.[5–8]

An alternative method of separating aerosol and cloud with use of SAGE II extinction data at two wavelengths, 1020 and 525 nm, was described by Kent and McCormick[9] and Kent *et al.*[3] The extinction produced by cloud particles is approximately equal at the two wavelengths, whereas the aerosol extinction is normally wavelength dependent. This difference in wavelength behavior is used to separate the two components. The paper by Kent *et al.* also contains a description of the validation of their model with data obtained by airborne lidar at the same time, and in the same atmospheric volume, as the SAGE II measurement. This comparison has enabled SAGE II cloud measurements to be interpreted in terms of the visual characteristics of the cloud. By virtue of the long horizontal path over which SAGE II makes its measurements, the extinction is extremely sensitive to the presence of thin cloud. A comparison of the SAGE II data with concurrent lidar data, and interpretation of the latter in visual terms, has shown that much of the SAGE II cloud data

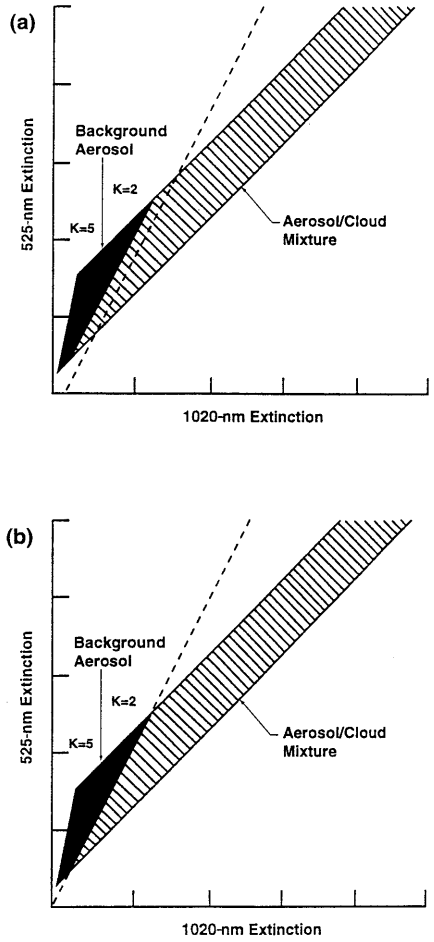

Fig. 1. Theoretical basis for two methods of separating aerosol and cloud in the SAGE II data set: (a) the slope and intercept method and (b) the slope method.

correspond to subvisual cirrus, and that the lowest extinction levels measurable are approximately 1 order of magnitude below those produced by cloud at the subvisual–visual threshold. Sassen *et al.*[10] and Sassen and Cho[11] described measurements made on subvisual cirrus clouds (optical thickness less than 0.03) similar to those viewed by SAGE II.

The method for separating aerosol and cloud used by Kent *et al.* (which is referred to here as the slope and intercept method) requires two input parameters that are determined from an extended aerosol–cloud data set. This method is illustrated in Fig. 1(a), which shows a plot of the expected relationship between the extinction at 525 nm and that at 1020 nm. The solid area in the figure indicates the location of data for cloud-free aerosol, where the ratio of the extinctions at the two wavelengths is assumed to lie between approximately 2 and 5. The shaded area indicates the expected extinctions when cloud as well as aerosol occurs along the optical path. The dashed line that separates the aerosol from the aerosol–cloud mixture is calculated from the distribution of data points within an ensemble. To obtain statistically meaningful values for the parameters of the dashed line, which depend on altitude, season, and degree of volcanic activity, a fairly large number of experimental data points must be accumulated. Typically a data ensemble consists of all data points obtained within a 3-month time segment, at 1-km-height intervals, and a 20° latitude band. Because the slope and intercept of this line are determined from an extended data set obtained about the time of each event to be classified, the method cannot be applied immediately to a current measurement.

The slope and intercept method is not the only method that has been used. Wang *et al.*[12] have used the ratio of extinction at 525 nm to that at 1020 nm to distinguish aerosol from cloud (this is referred to here as the slope method). This method, which is illustrated in Fig. 1(b), is similar to the slope and intercept method but somewhat simpler, the line separating the aerosol from the aerosol–cloud mixture passing through the origin. In this method, the slope can also be determined from the data subset itself or from a constant value chosen. Wang *et al.* studied tropical aerosol and cloud data for 1 year and used a constant slope of 2.1. The advantage of using a constant value lies in the fact that a data accumulation (typically for 3 months) is not required. Against this must be set the fact that determination of the slope, or slope and intercept, from appropriate subsets of a global data ensemble can be expected to provide better values for these constants. In the analysis presented below we determine the parameters for the slope and intercept method from the actual data sets used; for the slope method we use a constant slope value of 2.0. The SAGE III methods considered use both constant and data-derived parameters.

Other methods have also been tried, based on cluster analysis[13] and on the presence of strong gradients in the aerosol extinction profile.[14] They have not been used extensively but may merit further exploration, particularly under conditions in which the more standard methods cannot be used. All the methods described become difficult or impossible to use at times of high volcanic activity. As a result of the injection of sulphur dioxide into the stratosphere, sulfuric acid aerosols are formed that are gradually distributed globally and transferred downward into the upper troposphere.[15] The largest aerosol particles formed in this way may have radii between 500 and 1500 nm.[16] Extinction values at the 525-nm and 1020-nm wavelengths are similar and cannot be readily distinguished. In addition, volcanic aerosols often form thin layers so that in their physical geometry they also resemble cloud. Volcanic aerosols are gradually lost from the stratosphere with an exponential decay time of the order of 1 year.[17] The length of time that an aerosol–cloud separation method is unreliable will depend on the magnitude of the volcanic eruption and its location and time relative to that of the measurement in question. In practice, following a major eruption such as that of Mount Pinatubo in June 1991, the data cannot be used for a period of 2 or 3 years. Aerosols can also

Table 1. Data Sources Used for Aerosol Extinction Simulations

Reference	Time Period	Altitude (km)	Latitude (°N)	Number of Measurements
Wilson *et al.*[21]	1988–1992	13–19	31–49	4
Snetsinger *et al.*[22]	1984–1986	16–18	~37	2
Oberbeck *et al.*[23]	1981–1982	18–22	27–42	6
Pueschel *et al.*[24]	1991	17–18	37	2
Knollenberg and Huffman[25]	1982–1983	13–21	33–50	13
Pueschel *et al.*[26]	1991–1992	11–21	26–89	54
Deshler *et al.*[16]	1991–1993	17	41	12
Goodman *et al.*[27]	1992–1993	14–19	37	12

reach the upper troposphere from the Earth's surface,[18] with a variety of compositions, sizes, and optical properties. Pueschel *et al.*[19] have shown, however, that the free troposphere (over the Pacific Ocean) is dominated by sulfur-containing aerosols and that the concentration of surface-derived materials falls off rapidly with altitude. These *in situ* observations are supported by satellite and lidar data, which show the downward descent of stratospheric aerosol into the upper troposphere.[18,20] In the present analysis we assume the upper troposphere and lower stratosphere to be dominated by aerosols whose principal chemical component is sulfuric acid.

3. Aerosol and Cloud Simulations

The proposed method for discriminating aerosol from cloud in SAGE III data uses the extinction data at wavelengths 525, 1020, and 1550 nm. To determine how this method will perform, and to intercompare it with existing methods used for the SAGE II data, simulation studies were carried out. As input to these simulations, over 100 *in situ* measured aerosol size distributions were taken from published literature and used to derive wavelength-dependent values for the aerosol extinction. These measurements cover the period 1981–1993, altitudes from the upper troposphere to the stratospheric layer maximum, and various levels of volcanic perturbation. Most data are recent postvolcanic, as the majority of research flights were made at those times, and a variety of *in situ* measurement techniques were used. The data sources and other relevant information are listed in Table 1.[16,21–27]

Mie theory[28] was used to calculate extinction cross sections for the various measured aerosol size distributions. We assumed that the aerosols consist of 75% solutions of sulfuric acid,[15] and corresponding refractive indices were used at each wavelength.[29–30] Cloud is variable in space and time and no attempt was made to simulate a range of cloud conditions. Nevertheless, to be able to compare quantitatively the relative performance of different cloud–aerosol separation methods, it was necessary to define the cloud distribution. As the main application of this data set is for high-altitude cloud, a cloud model was taken that is typical of the altitude. The model

Table 2. Cloud Occurrence Frequency Used in Simulations[a]

Cloud Extinction (10^{-6} m^{-1})	Occurrence Frequency[b]
1	0.11
2	0.04
3	0.03
4	0.02
5	0.02
6	0.02
7	0.02
8	0.02
9	0.01
10	0.01
11	0.01
12	0.01
13	0.01
14	0.01
15	0.01
16	0.01
17	0.01
18	0.01
19	0.01
20	0.00
	Total 0.39

[a]SAGE II, 20 °N to 20 °S, 16.5-km altitude.
[b]For a single event at the altitude and location shown.

taken was derived from 1988 (a volcanically quiet year) SAGE II measurements taken at low latitudes (20 °S to 20 °N) at an altitude of 16.5 km. This cloud distribution, which in practice is continuous, was discretized in units of 1.0×10^{-6} m^{-1}. This unit is a few times greater than the extinction of background aerosol at a wavelength of 1020 nm but considerably less than that due to the El Chichón or Mount Pinatubo volcanic aerosol. The frequency of different cloud extinction levels is shown in Table 2 (note that the total probability of cloud being observed is approximately 40%). These values are zonal averages and are expressed as the probability of the cloud extinction falling within a given range for a single SAGE II or SAGE III measurement. We assumed that no wavelength variation occurs in this extinction (the measured values were obtained at a wavelength of 1020 nm). Clearly these values are not typical of other altitudes or applicable to specific locations, but we use them in conjunction with the aerosol extinction values calculated from *in situ* aerosol measurements to determine the error frequency of different aerosol–cloud separation methods. Because the cloud frequency at the altitude chosen is low, error rates at times of volcanic injection are likely to be high. Lower error rates normally apply at lower altitudes where the cloud occurrence frequency is higher and volcanic contamination is less. The fact that the error rates are attitude dependent should not affect intercomparison of the performance of different aerosol–cloud separation methods, where we are concerned with relative rather than absolute effectiveness.

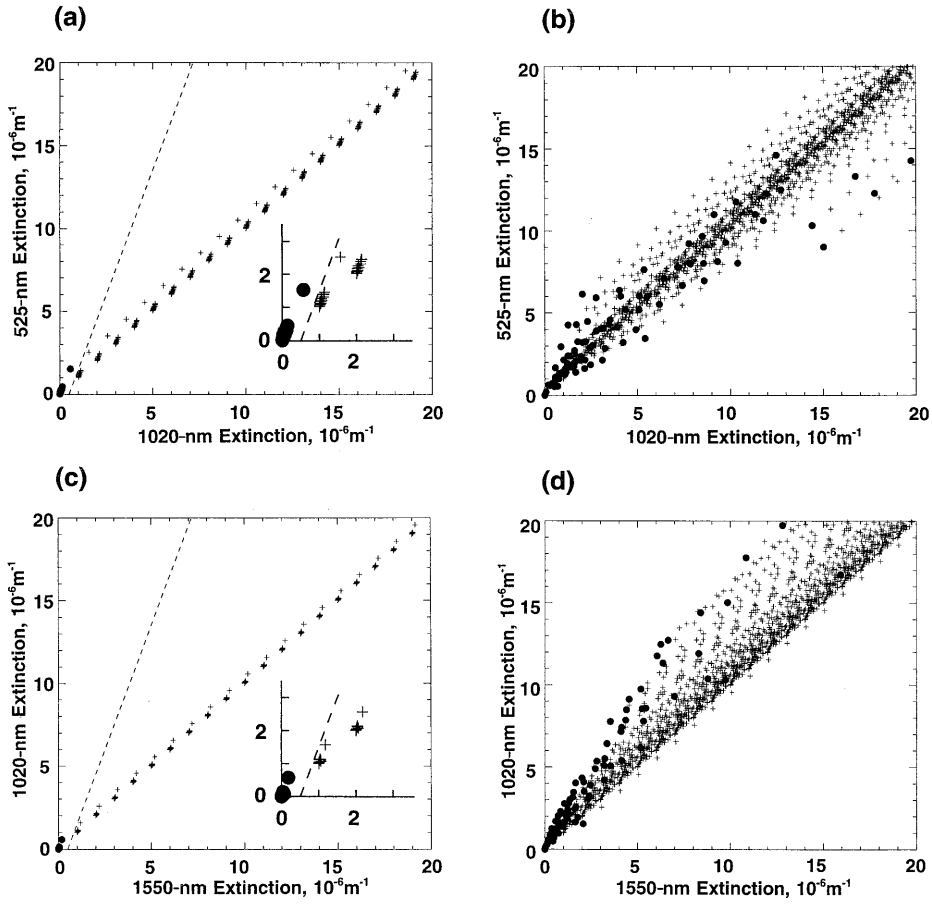

Fig. 2. Scatterplots showing the relationships between the simulated extinctions at 525, 1020, and 1550 nm. Filled circles correspond to aerosol data only; crosses correspond to aerosol plus different amounts of simulated cloud. The dashed lines demarcate aerosol and cloud in panels (a) and (c). (a) Background, 525 nm versus 1020 nm; (b) volcanically perturbed, 525 nm versus 1020 nm; (c) background, 1020 nm versus 1550 nm; (d) volcanically perturbed, 1020 nm versus 1550 nm. Inserts in (a) and (c) show enlarged views of the regions of these plots near the origin.

Figures 2(a) and 2(b) depict scatterplots of modeled aerosol extinction values at 525 and 1020 nm, shown by filled circles, and aerosol plus cloud extinction values, shown by crosses. No attempt was made to include error bars in this figure. SAGE II relative errors for cloud-free aerosol extinction at tropopause altitudes are 5–10% at 1020 nm and 10–20% at 525 nm. These values increase to 10–30% at both wavelengths when cloud is present. We divided the data into two classes: (a) background, which excludes the volcanically perturbed time periods within 2 years of the eruption of either El Chichón (April 1982) or Mount Pinatubo (June 1991) (11 measurements), and (b) the volcanically perturbed time periods (94 measurements). These two classes are shown respectively in Figs. 2(a) and 2(b). In Fig. 2(a) a clear distinction is shown between the aerosol data points and the cloud-contaminated data points that are demarcated by the dashed line. This demarcation is not possible in Fig. 2(b), where the data points show a strong overlap. Figures 2(c) and 2(d) show similar scatterplots for the extinctions at 1020 and 1550 nm. The demarcation in Fig. 2(c) is quite clear. Although the demarcation in Fig. 2(d) is better than that shown in Fig. 2(b), considerable overlap appears between the aerosol and the aerosol plus cloud data points.

Care must be taken in the interpretation of the 100% success rate shown for the aerosol–cloud demarcation in Figs. 2(a) and 2(c). The degree of success is dependent on the size of the units into which the cloud extinction is discretized. If the unit chosen was smaller, some (small) overlap could have occurred between the aerosol and the aerosol plus cloud data points where the cloud extinction is low. A few large ice particles occurring at some point along the optical path can be identified technically as a cloud, but they would produce a low extinction that would not be distinguishable above the extinction that is due to the aerosol background. The frequency with which such situations arise is not known; radiatively, these situations are not of great significance.

4. Simulation Studies for SAGE III Wavelengths

The theoretical basis for the method that we propose for use with the SAGE III data is shown in Fig. 3. Figure 3(a) depicts a plot of the 525-nm/1020-nm extinction ratio versus the 1020-nm/1550-nm extinction ratio calculated for narrow rectangular aerosol size distributions (mean radius r_0 and width dr_0, where $dr_0/r_0 = 10^{0.025}$, i.e., $dr_0/r_0 \sim 0.06$) for which the composition is assumed to be 75% sulphuric acid. Numbers adjacent to the solid curves give the particle radii in micrometers; Figs. 3(a) and 3(b) are identical except for a scale change. Cloud (not mixed with aerosol) is shown by a filled circle at location (1.0, 1.0). Mie calculations show that, for spherical ice particles with radii greater than 4 μm, both 525-nm/1020-nm and 1020-nm/1550-nm extinction ratios lie between

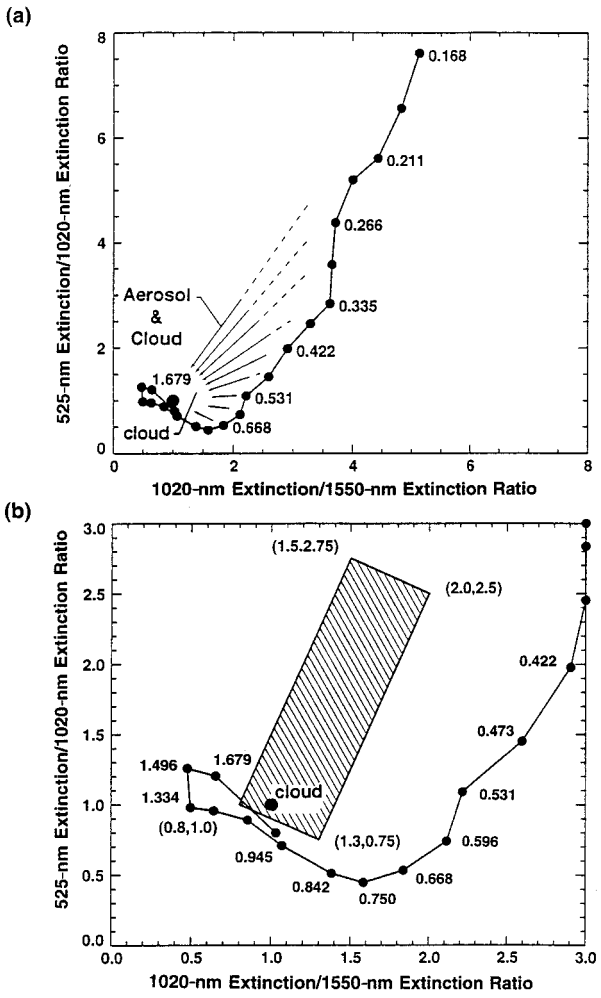

Fig. 3. Theoretical basis for the proposed method of separating aerosol and cloud in the SAGE III data set. The solid curves indicate the relationship between the 525-nm/1020-nm and the 1020-nm/1550-nm extinction ratios for narrow rectangular size distributions. Calculations were made for a 75% sulphuric acid composition. Numbers adjacent to the solid curves show the particle radii in micrometers. Cloud undiluted by aerosol is shown by the filled circle at location (1.0, 1.0). (a) and (b) show the same data plotted to different scales; data points within the shaded area in (b) are considered to correspond to cloud as well as aerosol along the optical path.

0.8 and 1.2, and that for particles with radii greater than 8 μm these ratios lie between 0.9 and 1.1. Increasing amounts of cloud added to aerosol cause the data points to move away from the aerosol curve and toward the (1.0, 1.0) point, as shown by the arrows in Fig. 3(a). The shaded area in Fig. 3(b) was chosen to delineate the region of the plot where the data may be supposed to be cloud. Data points outside this area were taken to be aerosol. The shape and size of this area was determined on the basis of the simulation studies. A parallelogram was chosen as a simple geometric shape surrounding the cloud point, with two boundaries between this point and the theoretical curve for the extinction ratios. We adjusted the locations of these two boundaries (bottom and right) to achieve optimum performance. The effect of adjusting these boundaries is discussed in Section 5 in conjunction with the reliability of aerosol or cloud identification. The exact positions of the other two edges of the parallelogram (top and left) are not critical. As shown below, under background aerosol conditions we found no major problems in the separation of the two constituents. Under volcanic conditions, exact separation is not possible. The area shown here represents a compromise between two error conditions. In the first error condition, the cloud subset contains additional noncloud data points that are due to the presence of large aerosols that have extinction values that are insensitive to wavelength. In the second error condition, cloud data points representing thin cloud occur outside this area; they are classified as aerosols and so are lost from the total cloud count.

Figures 4(a) and 4(b) depict scatterplots of the 525-nm/1020-nm extinction ratio versus the 1020-nm/1550-nm extinction ratio for the background and volcanic situations, respectively. As in Fig. 2, the aerosol data points are shown by solid circles, those with added cloud by crosses. It can be seen that, although these calculations are for real aerosol size distributions, the distribution of aerosol extinction ratios is similar to that for the narrow rectangular size distributions shown in Fig. 3. Nevertheless, some scatter is present in the data values in Figs. 4(a) and 4(b) because of the continuous nature of real aerosol size distributions and the possible occurrence of more than one mode within a single size distribution. As in Fig. 3, the same data are shown with different scales in Figs. 4(a) and 4(b) and Figs. 4(c) and 4(d). Figures 4(c) and 4(d) depict the area chosen for the selection of cloud data as in Fig. 3(b). In the case of the nonvolcanic aerosol size distributions shown in Figs. 4(a) and 4(c), and the discrete cloud distribution used here, complete separation of aerosol and cloud occurs. For the volcanic aerosol shown in Figs. 4(b) and 4(d), the separation is incomplete, and it is clear from the overlap between the aerosol data points and the aerosol plus cloud data points that no perfect separation is achievable. Small movements of the boundaries of the shaded area change the error rate within the two error classes discussed above, but make little change to the total error rate (see Section 6 for further discussion).

5. Simulation Results

Performance intercomparisons were made between the following five methods for separating aerosol and cloud:

1. The three-wavelength method described in Section 4 (with data at 525, 1020, and 1550 nm; see Figs. 3 and 4).
2. The slope method [with data at 525 and 1020 nm; see Fig. 1(b)]: a value of 2.0 was chosen for the 525-nm/1020-nm extinction ratio used to separate aerosol and cloud.

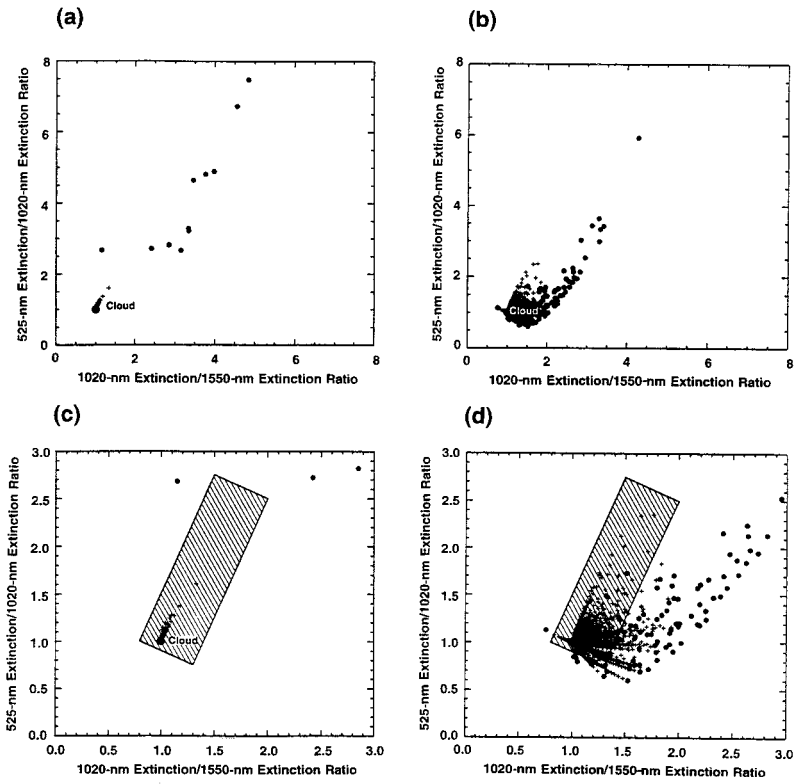

Fig. 4. Scatterplots of the 525-nm/1020-nm and the 1020-nm/1550-nm extinction ratios for *in situ* measured size distributions during background and volcanically perturbed conditions. Solid circles correspond to aerosol data only; crosses correspond to aerosol plus different amounts of simulated cloud. Plot scales and the shaded area, which are used to determine the presence of cloud, are the same as in Fig. 3. (a) and (c) background, plotted to different scales; (b) and (d) volcanically perturbed, plotted to different scales.

3. The slope and intercept method [with data at 525 and 1020 nm; see Figs. 1(a), 2(a), and 2(b)]: optimum values for the slope and intercept were determined from the data subsets.

4. The slope method (with data at 1020 and 1550 nm): a value of 1.5 was chosen for the 1020-nm/1550-nm extinction ratio used to separate aerosol and cloud.

5. The slope and intercept method [with data at 1020 and 1550 nm; see Fig. 2(c) and 2(d)]: optimum values for the slope and intercept were determined from the data subsets. Methods (2) and (3) are those described above as having been used with SAGE II data. Methods (4) and (5) are essentially the same as (2) and (3) but employ the extinctions measured at the two longest SAGE III wavelengths only.

Errors in the cloud occurrence rates found as a result of these discrimination methods can be of two types: *cl* denotes a loss of true cloud data points from the subset identified as cloud; *ag* denotes an increase in the apparent number of cloud data points as a result of the inclusion into that subset of unwanted contaminating aerosol points. To provide a quantitative measure of the success of a method a total error rate *er* is defined as

$$er = (cl^2 + ag^2)^{0.5}.$$

The three error measurement rates *er*, *cl*, and *ag* can be expressed as fractions or percentages of the true cloud amount in the subset.

The results of this analysis are shown in Table 3.

Table 3. Cloud Identification Error Rate as a Function of Method and Aerosol State

Method	Aerosol Condition	Cloud Loss Rate (%)	Contamination Rate (%)	Overall Error Rate (%)
(1) Three-wavelength method	Background	0.0	0.0	0.0
	Volcanic	21.7	19.1	28.9
(2) Slope (2.0) method (525 and	Background	0.0	0.0	0.0
1020 nm)	Volcanic	1.0	220.0	221.0
(3) Slope and intercept method	Background	0.0	0.0	0.0
(525 and 1020 nm)	Volcanic	56.4	32.7	65.2
(4) Slope (1.5) method (1020 and	Background	0.0	23.3	23.3
1550 nm)	Volcanic	14.6	49.1	51.2
(5) Slope and intercept method	Background	0.0	0.0	0.0
(1020 and 1550 nm)	Volcanic	34.2	21.8	40.6

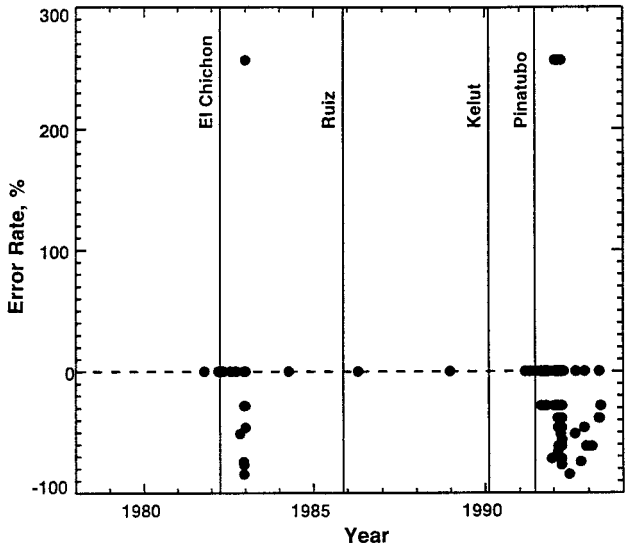

Fig. 5. Cloud identification error rate as a function of time of measurement. Each data point represents one *in situ* measurement; most measurements were made at times following volcanic activity. The concentration of errors during the periods following the eruptions of El Chichón and Mount Pinatubo is outstanding.

The values shown for the error rate of each method are the lowest that we found for any values of the parameters where these are variable and potentially determinable from within the data set (methods 3 and 5). These performance intercomparisons were carried out separately for background and volcanically perturbed conditions. Conclusions to be drawn from this table are as follows:

1. Methods (1), (2), (3), and (5) all work well with background aerosols.
2. Method (2) shows large errors when volcanic aerosols are present, which is to be expected. The constant slope value of 2.0 is applicable to background aerosols within a single year (1989) and not suitable for volcanic conditions. A better slope value could be found, but the performance of the method is not likely to be better than that of the slope and intercept method (3). Methods (3), (4), and (5) all show error rates in the range 40–60%. [The same comments made with respect to method (2) also apply to method (4).] Of these three methods, the best is the slope and intercept method with use of the longer two wavelengths of SAGE III.
3. The best results are obtained with method (1) with wavelengths 525, 1020, and 1550 nm.

The error rates achievable with method (1) during volcanic conditions, even though they are lower than those shown for the other methods, may still be unacceptably high for many purposes. Such conditions do not last for a great length of time after an eruption. The duration of these conditions is illustrated in Fig. 5, which shows the cloud identification error rate as a function of time between 1982 and 1993. Each point in these plots represents one *in situ* measurement (some overlap of the data points occurs in this figure). Incorrect interpretation of an aerosol data point as cloud causes a positive cloud error for that data point. The magnitude of the error is 100/(total simulated cloud frequency) ~250%. Similar incorrect interpretation of cloud as aerosol can cause an error between 0% and −100%, the magnitude of the error depending on the fraction of the simulated cloud that falls outside the designated cloud area. Errors of both types (cloud loss and cloud contamination) commenced a few months after the eruptions of El Chichón and Mount Pinatubo and were maximized after a delay of approximately 1 year. As can be seen in the post-Mount Pinatubo data, recovery then began. In the case of El Chichón, data taken 2 years and longer after the eruption showed no ambiguities. Care must be taken when global conclusions are made from this plot as the data are localized and north of 31 °N.

6. Effect of Changing Cloud Selection Area

After a volcanic eruption, it is not possible to obtain an unambiguous separation of aerosol and cloud. Even with the three-wavelength method, cloud loss and contamination rates measure approximately 20%. These rates can be altered by one shifting the boundaries of the area used to identify the presence of cloud. This modification is illustrated in Fig. 6, which shows the effects of shifting the location of the edge of the identifying parallelogram where the majority of the ambiguity occurs. The dashed lines in Fig. 6(a) indicate the different positions of the edge for which calculations were carried out, the positions of the edge being specified by the coordinates of its upper and lower ends. The results of this operation as they affect the loss and contamination rates are shown in Fig. 6(b) and Table 4; the figure and table also show the effects on aerosol identification. The results can be summarized qualitatively as follows:

1. As the selection area is decreased (large *ycc*), the rate of corruption of cloud by volcanic aerosol decreases while the loss rate of cloud increases.
2. As the selection area increases (small *ycc*), the rate of corruption of aerosol by cloud decreases while the aerosol loss rate increases.
3. Shifting the boundary can clearly be used to reduce the effect of corruption of either aerosol or cloud by the other. An unfortunate aspect of these results is that, in both cases, as we achieve a greater certainty of the component that we are identifying, the loss rate of that component is found to increase even faster. Thus reducing the cloud corruption rate from 20% with a concurrent loss rate of 20%, to a cloud corruption rate of 10%, raises the loss rate to approximately 50%.
4. The algorithm performance for aerosol identification shown in Table 4 is better than that for cloud. The relative performance is dependent on the amount of cloud present and, under conditions of increased cloudiness, could be biased in the opposite direction.

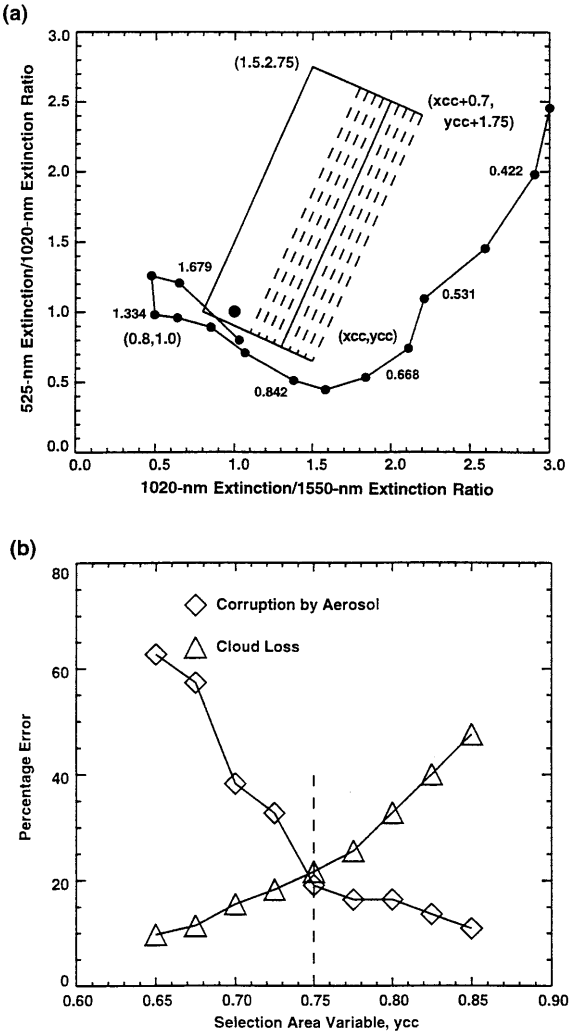

Fig. 6. (a) Alternative cloud selection areas for which simulations were carried out. The coordinates of the ends of the dashed lines are given in Table 4. (b) Effect of changing the cloud selection area, as shown in (a), on cloud loss and corruption rates under volcanic conditions.

5. The calculations described are for the atmospheric conditions encountered within 2 years of the eruptions of El Chichón and Mount Pinatubo. Examination of the effect of changing the area boundaries as described, for background aerosol conditions, indicates no change in algorithm performance.

7. Effects Resulting from the Inhomogeneous Nature of Cloud

A basic assumption in the inversion scheme used to obtain the vertical profile of aerosol extinction is that the atmospheric constituents are horizontally stratified.[31] Although this is an acceptable assumption for stratospheric aerosol, and possibly for tropospheric aerosol as well, it is clearly not true for cloud. In their statistical intercomparison of the SAGE II and the International Satellite Cloud Climatology Project cloud data sets, Liao *et al.*[32] deduced a mean horizontal cloud size of 75 km. More-recent unpublished studies using lidar data have indicated a size even smaller. For the assumption of horizontal homogeneity to be valid, the cloud should be homogeneous and uniform for a major part of the tangent path through the relevant part of the atmosphere, typically several hundred kilometers. This assumption clearly is not true, even for the higher-altitude cloud that SAGE II and SAGE III most readily detect. Simulation studies show at least three significant effects of the inhomogeneous nature of cloud on the solar occultation data. The first is that an error may be present in the identified cloud altitude. For example, if cloud occurs to one side of the tangent point it will be assigned to the tangent altitude, which is less than the true altitude. The second effect is that, because of the flattened shape of much high-altitude cloud, the ray path through such a cloud will be less than if it had occurred at the tangent point. The shorter ray path will result in a lower apparent extinction. A third effect that occurs is to the inverted extinction value just below the cloud. The inversion scheme assumes that the cloud is uniform along the ray path and that any ray path whose tangent point is lower than that at which the cloud is detected must pass through the cloud. Passage through the cloud will often not occur if the cloud is nonuniform, or it is small and isolated. Inverted values for lower altitudes, particularly those just below the cloud, will be too low and may sometimes even be negative if permitted by the inversion. Studies have yet to be made of the influence of these effects on the aerosol–cloud separation schemes we describe in this paper.

Table 4. Results of Modifying Cloud Selection Area in Aerosol–Cloud Separation Algorithm[a]

xcc	*ycc*	Aerosol Corruption Rate (%)	Aerosol Loss Rate (%)	Cloud Corruption Rate (%)	Cloud Loss Rate (%)
1.10	0.850	18.6	4.3	10.9	47.6
1.15	0.825	15.6	5.3	13.6	40.0
1.20	0.800	12.8	6.4	16.4	32.8
1.25	0.775	10.0	6.4	16.4	25.6
1.30	0.750	8.5	7.4	19.1	21.7
1.35	0.725	7.1	12.8	32.7	18.3
1.40	0.700	6.0	14.9	38.2	15.5
1.45	0.625	4.4	22.3	57.3	11.4
1.50	0.650	3.8	24.5	62.7	9.7

[a]Volcanic conditions only.

8. Summary

Simulation studies have been made on several methods of distinguishing aerosol from cloud in the SAGE II and SAGE III data sets. These include a proposed method that will use the additional long-wavelength extinction information that will be available from SAGE III. Under nonvolcanic conditions both SAGE II and SAGE III can provide good discrimination between aerosol and cloud. Under volcanically perturbed conditions the error rate with use of the proposed SAGE III method is less than half that ob-

tained with the common SAGE II method. The discrimination method selected for use with SAGE III data uses the extinction at three wavelengths, 525, 1020, and 1550 nm, and is thus limited to the altitude range over which these data are likely to be available (above 6 km). Several avenues for future study present themselves:

1. Minor modifications to the currently proposed method involves slight changes to the defined boundaries that delineate aerosol from cloud. Some improvement may be possible but it is not likely to be significant; absolute discrimination under volcanically perturbed conditions is not possible with the SAGE III wavelengths discussed here.
2. Incorporation of extinction information at other wavelengths between 525 and 1020 nm. At altitudes above 6 km, it is unlikely that this method will produce much better discrimination than the current method, as the extinctions at the additional wavelengths will contribute little particle size information that is not contained in the extinctions from the three wavelengths already used. Below 6 km, the situation is quite different. Data will most likely not be available at 525 nm. Use of data at the slightly longer wavelengths (currently set at 757 and 872 nm) that will be available will almost certainly be beneficial.
3. Use of quite different discrimination techniques such as searching for steep vertical gradients in extinction as would be produced by most cloud. These techniques offer interesting possibilities, particularly at lower altitudes where the multiwavelength information is limited. Again, we note that, in the upper troposphere and lower stratosphere, fresh volcanic material can also occur in thin, intense layers.
4. Use of SAGE III transmission profiles that are derived prior to the inversion process. Inversion causes some of the information on inhomogeneities and extinction gradients to be lost.

We thank the many people who read and commented on the analysis presented in this paper, including members of the SAGE III Science Team. Particular thanks are due to E. Shettle of the Naval Research Laboratory and G. Vali of the University of Wyoming. This research was supported under NASA contract NAS1-18941.

References and Notes

1. M. P. McCormick, W. P. Chu, J. M. Zawodny, L. E. Mauldin, and J. R. McMaster, "Stratospheric Aerosol and Gas Experiment III (SAGE III), aerosol and trace gas measurements from Earth Observing System (EOS)," in *Remote Sensing of Atmospheric Chemistry*, J. L. McElroy and R. J. McNeal, eds., Proc. SPIE **1491,** 125–141 (1991).
2. M. P. McCormick, J. M. Zawodny, W. P. Chu, J. W. Baer, J. Guy, and A. Ray, "Stratospheric Aerosol and Gas Experiment III (SAGE III)," in *Sensor Systems for the Early Earth Observing System Platforms*, W. L. Barnes, ed., Proc. SPIE **1939,** 137–147 (1993).
3. G. S. Kent, D. M. Winker, M. T. Osborn, and K. M. Skeens, "A model for the separation of cloud and aerosol in SAGE II occultation data," J. Geophys. Res. **98,** 20725–20735 (1993).
4. M. P. McCormick and R. E. Veiga, "SAGE II measurements of early Mount Pinatubo aerosols," Geophys. Res. Lett. **19,** 155–158 (1992).
5. G. E. Woodbury and M. P. McCormick, "Global distributions of cirrus clouds determined from SAGE data," Geophys. Res. Lett. **10,** 1180–1183 (1983).
6. G. E. Woodbury and M. P. McCormick, "Zonal and geographical distribution of cirrus clouds determined from SAGE data," J. Geophys. Res. **91,** 2775–2785 (1986).
7. E. W. Chiou, M. P. McCormick, W. P. Chu, and G. K. Yue, "Distributions of cirrus determined from SAGE II occultation measurements between November 1984 and October 1988," presented at the Conference on Cloud Physics, American Meteorological Society, San Francisco, Calif., 23–27 July 1990.
8. G. S. Kent, E. R. Williams, P.-H. Wang, M. P. McCormick, and K. M. Skeens, "Surface temperature related variations in tropical cirrus cloud as measured by SAGE II," J. Clim. **8,** 2577–2594 (1995).
9. G. S. Kent and M. P. McCormick, "Separation of cloud and aerosol in two-wavelength satellite occultation data," Geophys. Res. Lett. **18,** 428–431 (1991).
10. K. Sassen, M. K. Griffin, and G. C. Dodd, "Optical scattering and microphysical properties of subvisual cirrus clouds, and climatic implications," J. Appl. Meterol. **28,** 91–98 (1989).
11. K. Sassen and B. S. Cho, "Subvisual-thin cirrus lidar dataset for satellite verification and climatological research," J. Appl. Meterol. **31,** 1275–1285 (1992).
12. P.-H. Wang, M. P. McCormick, L. R. Poole, W. P. Chu, G. K. Yue, G. S. Kent, and K. M. Skeens, "Tropical high cloud characteristics derived from SAGE II extinction measurements," Atmos. Res. **34,** 53–83 (1994).
13. E. W. Chiou, Science Applications International Corporation, Hampton, Va. 23666 (personal communication, 1993).
14. R. E. Veiga, Science Applications International Corporation, Hampton, Va. 23666 (personal communication, 1993).
15. J. Rosen and V. A. Ivanov, "Stratospheric aerosols," in *Aerosol Effects on Climate*, S. G. Jennings, ed. (University of Arizona, Tucson, 1993).
16. T. Deshler, B. J. Johnson, and W. R. Rozier, "Balloonborne measurements of Mount Pinatubo aerosol during 1991 and 1992 at 41 °N: vertical profiles, size distribution, and volatility," J. Geophys. Res. **20,** 1435–1438 (1993).
17. G. K. Yue, M. P. McCormick, and E. W. Chiou, "Stratospheric aerosol optical depth observed by the Stratospheric Aerosol and Gas Experiment II: decay of the El Chichón and Ruiz volcanic perturbations," J. Geophys. Res. **96,** 5209–5219 (1991).
18. G. S. Kent, P.-H. Wang, M. P. McCormick, and K. M. Skeens, "Multiyear Stratospheric Aerosol and Gas Experiment II measurements of upper tropospheric aerosol characteristics," J. Geophys. Res. **98,** 20725–20735 (1995).
19. R. F. Pueschel, J. M. Livingston, G. V. Ferry, and T. E. DeFelice, "Aerosol abundances and optical characteristics in the Pacific basin free troposphere," Atmos. Environ. **28,** 951–960 (1994).
20. M. J. Post, C. J. Grund, A. O. Langford, and M. H. Profitt, "Observations of Mount Pinatubo ejecta over Boulder, Colorado by lidars of three different wavelengths," Geophys. Res. Lett. **19,** 195–198 (1992).
21. J. C. Wilson, H. H. Jonsson, C. A. Brock, D. W. Toohey, L. M. Avalone, D. Baumgardner, J. E. Dye, L. R. Poole, D. C. Woods, R. J. DeCoursey, M. Osborn, M. C. Pitts, K. K. Kelly, K. R. Chan, G. V. Ferry, M. Loewenstein, J. R. Podolske, and A. Weaver, "In situ observations of aerosol and chlorine monoxide after the eruption of Mount Pinatubo: effects of reactions on sulfate aerosol," Science **261,** 1140–1143 (1993).

22. K. G. Snetsinger, R. F. Pueschel, and G. V. Ferry, "Diminished effects of El Chichón on stratospheric aerosols, early 1984 to late 1986," Atmos. Environ. **26A,** 2947–2951 (1992).
23. V. R. Oberbeck, E. F. Danielsen, K. G. Snetsinger, and G. V. Ferry, "Effect of the eruption of El Chichón on stratospheric aerosol size and composition," Geophys. Res. Lett. **10,** 1021–1024 (1983).
24. R. F. Pueschel, S. A. Kinne, P. B. Russell, K. G. Snetsinger, and J. M. Livingstone, "Effects of the 1991 Mount Pinatubo volcanic eruption on the physical and radiative properties of stratospheric aerosols," in *IRS '92: Current Problems in Atmospheric Radiation*, S. Keevallik and O. Kärner, eds. (A. Deepak, Hampton, Va., 1993).
25. R. G. Knollenberg and D. Huffman, "Measurements of the aerosol size distribution in the El Chichón cloud," Geophys. Res. Lett. **10,** 1025–1028 (1983).
26. R. F. Pueschel, P. B. Russell, D. A. Allen, G. V. Ferry, K. G. Snetsinger, and J. M. Livingston, "Physical and optical properties of the Mount Pinatubo volcanic aerosol: aircraft observations with impactors and a sun-tracking photometer," J. Geophys. Res. **99,** 12915–12922 (1994).
27. J. Goodman, K. G. Snetsinger, R. F. Pueschel, G. Ferry, and S. Verma, "Evolution of Mount Pinatubo aerosol near 19-km altitude over western North America," Geophys. Res. Lett. **21,** 1129–1132 (1994).
28. C. E. Bohren and D. R. Huffman, *Absorption and Scattering of Light by Small Particles* (Wiley, New York, 1983).
29. K. F. Palmer and D. Williams, "Optical constants of sulfuric acid: application to the clouds of Venus?," Appl. Opt. **14,** 208–219 (1975).
30. It is recognized that the Palmer and Williams refractive-index values are for room temperature and that an appropriate temperature correction[33] should be made. Errors arising from the omission of this correction are likely to be smaller than those arising from the lack of exact knowledge of the aerosol composition and the measurement errors in the size distributions.
31. W. P. Chu, M. P. McCormick, J. Lenoble, C. Brogniez, and P. Pruvost, "SAGE II inversion algorithm," J. Geophys. Res. **94,** 8339–8351 (1989).
32. X. Liao, W. B. Rossow, and D. Rind, "Comparison between SAGE II and ISCCP high-level clouds. Part 1: Global and zonal mean cloud amounts," J. Geophys. Res. **100,** 1121–1185 (1995).
33. G. K. Yue, M. P. McCormick, and W. P. Chu, "Retrieval of composition and size distribution of stratospheric aerosols with the SAGE II satellite experiment," J. Atmos. Ocean. Technol. **3,** 371–380 (1986).